

Supporting Information

Creation of ordered 3D tubes out of DNA origami lattices

Johannes M. Parikka^a, Heini Järvinen^a, Karolina Sokołowska^a, Visa Ruokolainen^b,
Nemanja Markešević^a, Ashwin K. Natarajan^c, Maija Vihinen-Ranta^b, Anton Kuzyk^c,
Kosti Tapio^{a*}, J. Jussi Toppari^{a*}

^a. University of Jyväskylä, Department of Physics and Nanoscience Center, Jyväskylä, Finland

^b. University of Jyväskylä, Department of Biological and Environmental Science and Nanoscience Center, Jyväskylä, Finland

^c. Department of Neuroscience and Biomedical Engineering, Aalto University, 00076 Aalto, Finland.

KEYWORDS DNA, Origami, monovalent cation, divalent cation, self-assembly, hierarchical, surface deposition.

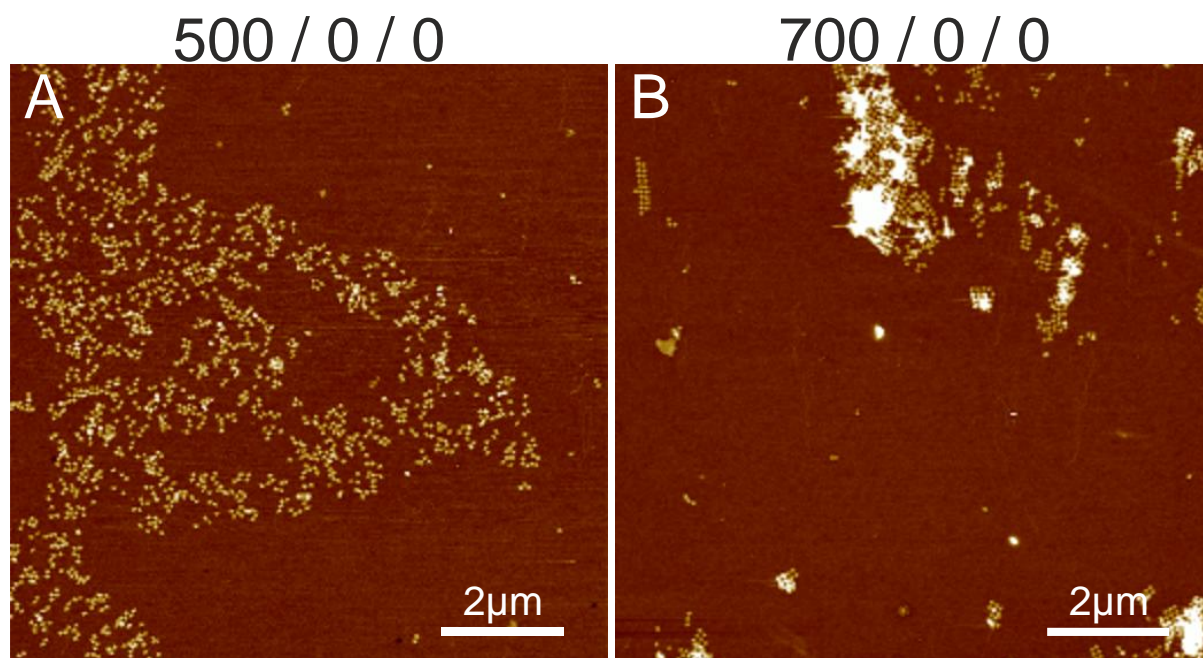


Figure S1. The effects of Mg^{2+} on lattice formation. The buffer conditions are listed on top of the images, where the concentrations are from left to right $C_{Mg^{2+}}$ / $C_{Ni^{2+}}$ / $C_{Na^{+}}$. (A) and (B) show AFM images of STs deposited in 1xTAE and either 500 mM or 700 mM $MgCl_2$ buffer, respectively.

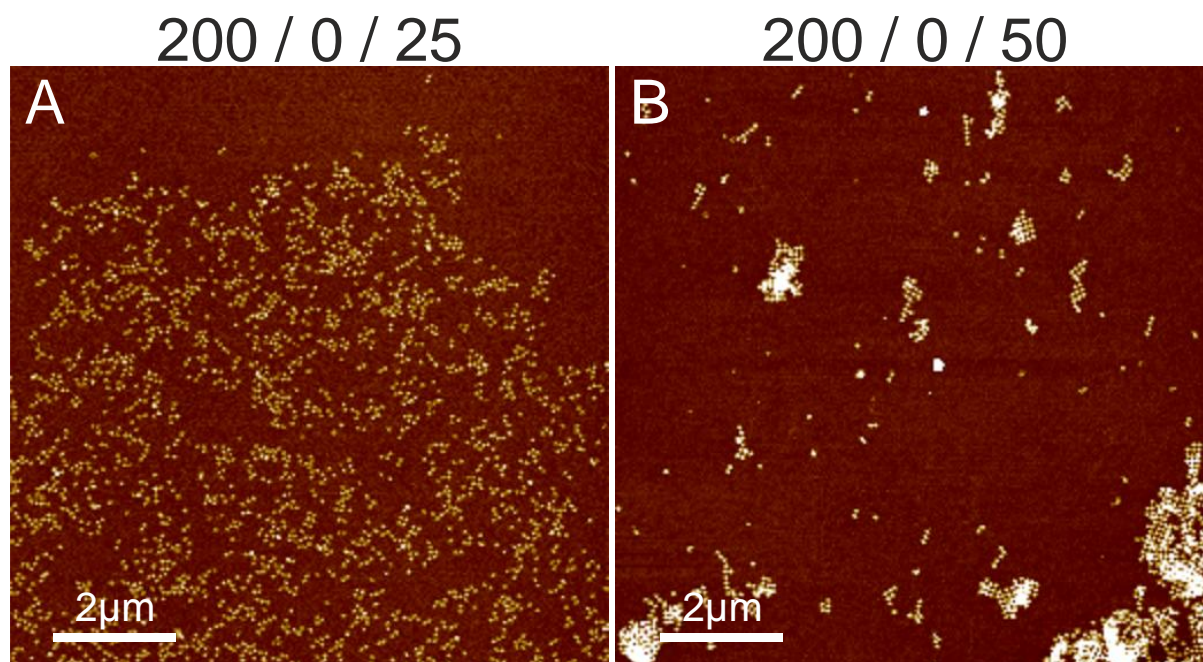


Figure S2. The effect of Na^{+} on lattice formation. The buffer conditions are listed on top of the images, where the concentrations are from left to right $C_{Mg^{2+}}$, $C_{Ni^{2+}}$ and $C_{Na^{+}}$, respectively. (A) and (B) show AFM images of ST deposited in 1xTAE where the concentration of Mg^{2+} is constant 200 mM and the concentration of Na^{+} is either 25 or 50 mM, respectively.

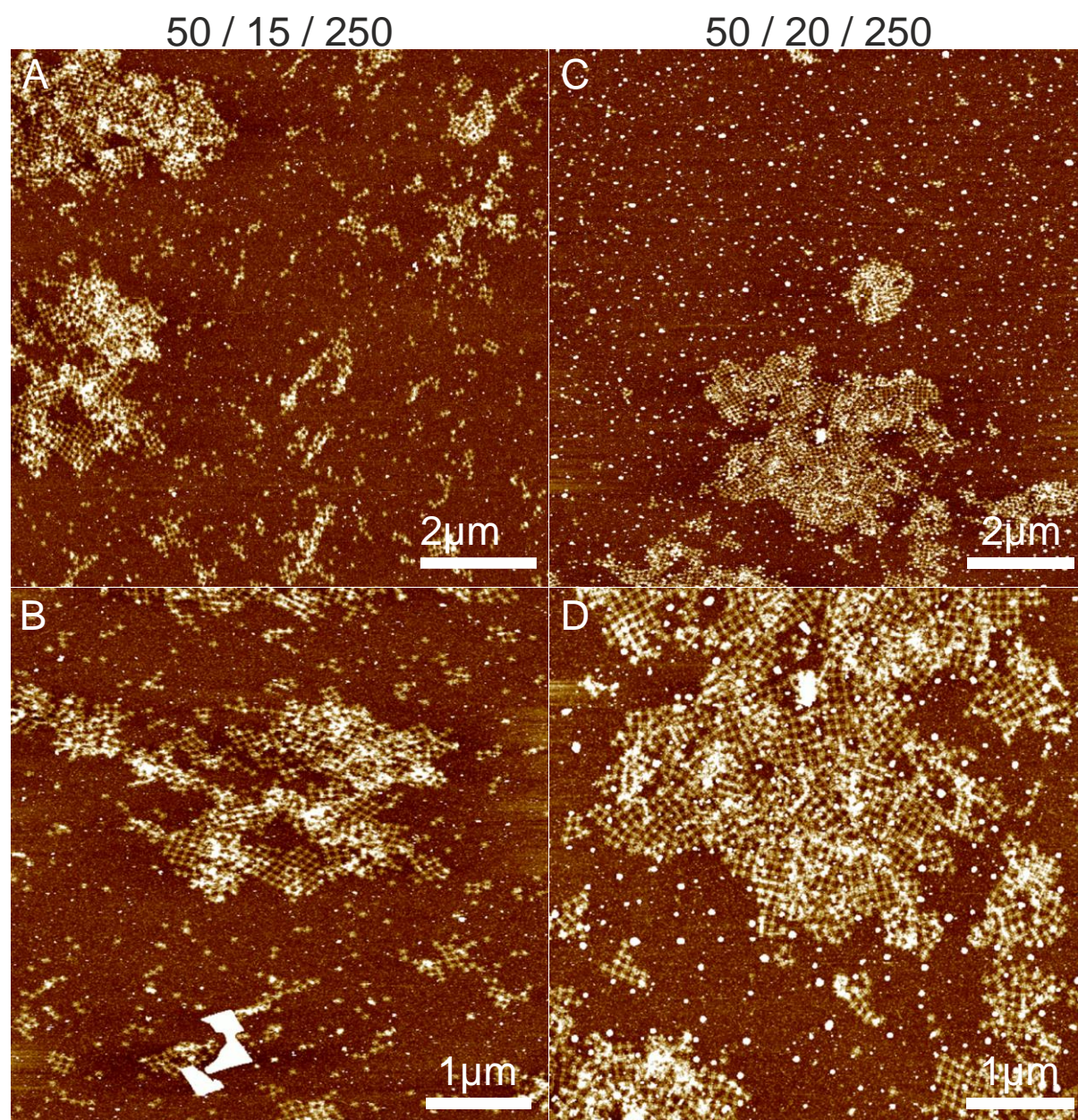


Figure S3. Extra AFM images of ST lattice formation, where excess Ni²⁺ causes aggregation. The buffer conditions are listed on top of the images, where the concentrations are from left to right $C_{Mg^{2+}} / C_{Ni^{2+}} / C_{Na^+}$. (A) and (B) show AFM images of STs deposited with 15 mM NiCl₂. (C) and (D) show AFM images of STs deposited with 20 mM NiCl₂.

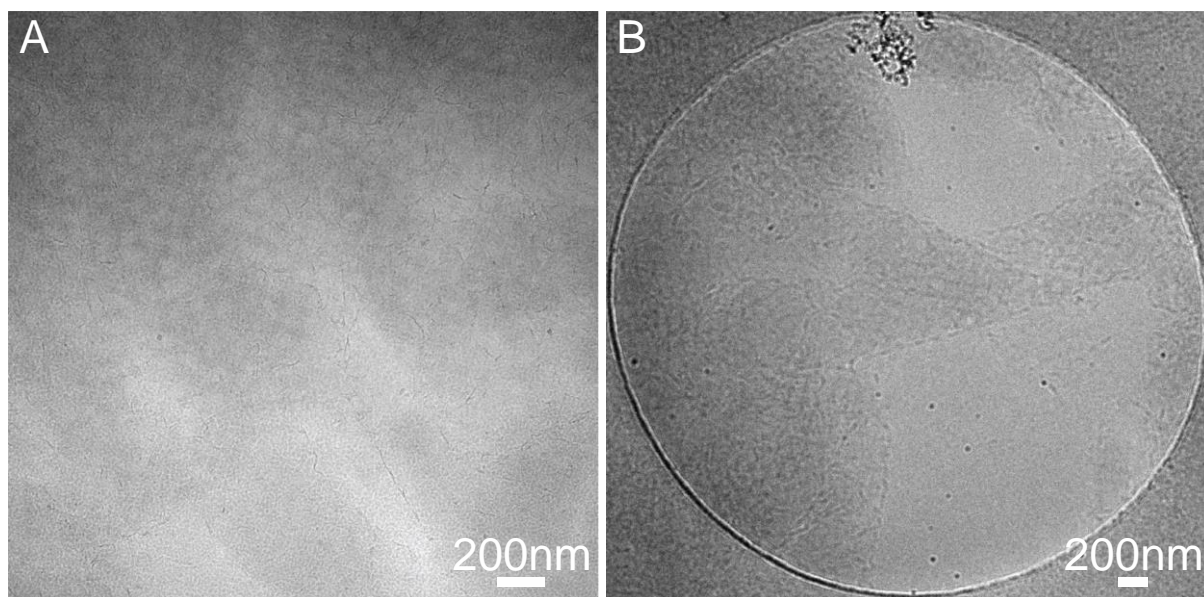


Figure S4. Extra cryo-TEM images of (A) 2D ribbons and (B) 3D tubes.

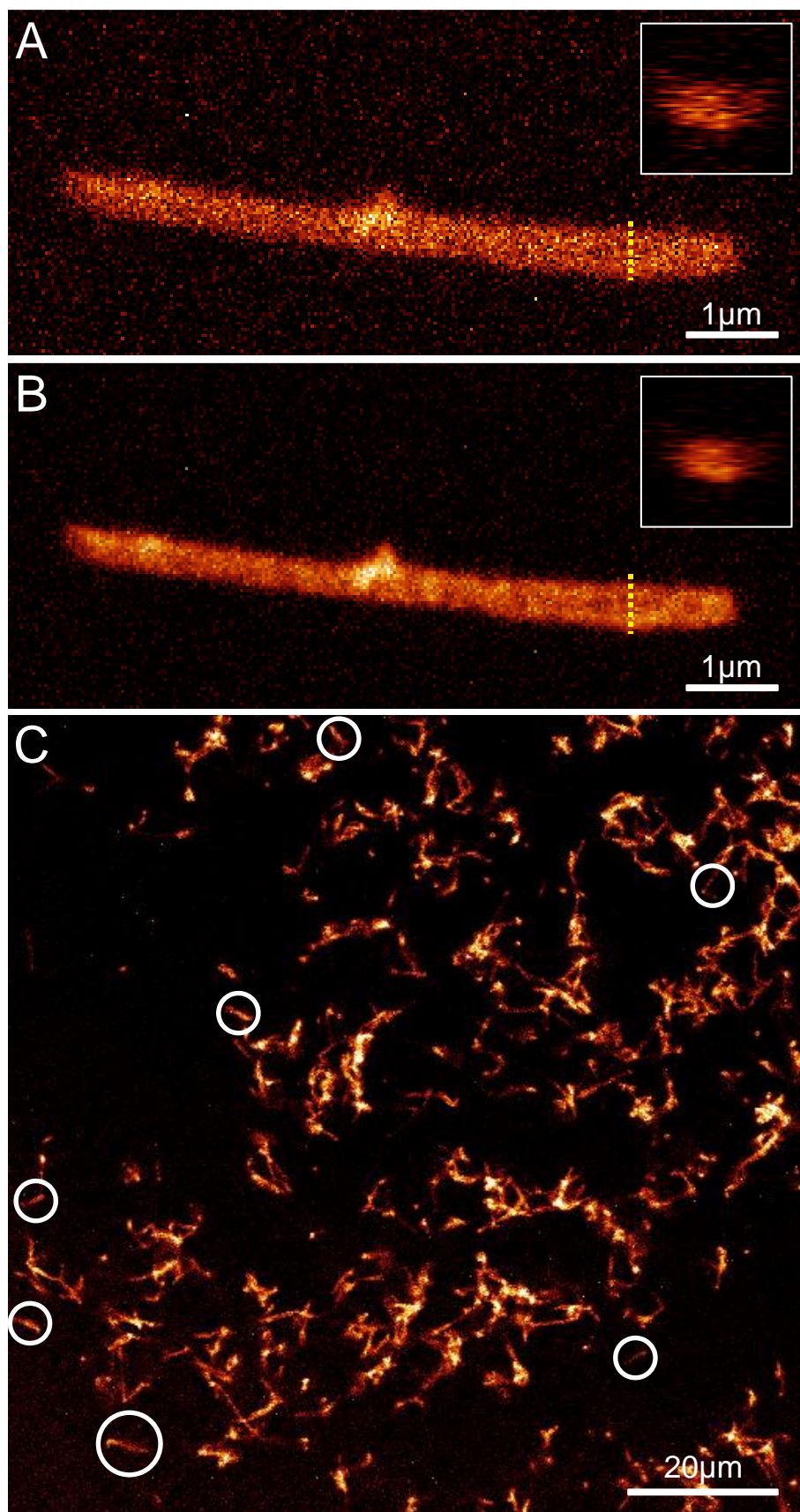


Figure S5. Extra confocal images of DNA origami tubes. (A) Non-processed confocal image of a tubes. The inset shows the cross section along the yellow, dashed line. (B) The same image as in A, but the original image is combined with a higher resolution deconvoluted version of the same image. We used Fiji and ImageJ -software for the deconvolution. The size of the inset images in A and B is $2\ \mu\text{m} \times 2\ \mu\text{m}$. (C) Overview of the confocal sample. Examples of separate tubes are highlighted with white circles.

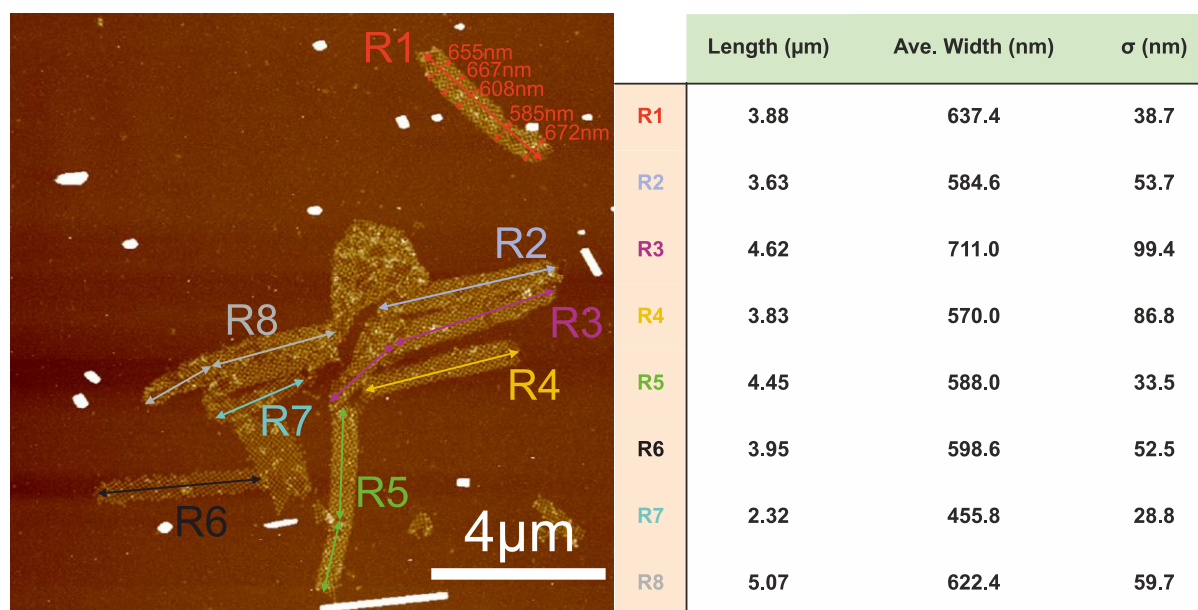


Figure S6. Example of an AFM image for the statistical analysis of the ribbon and tube dimensions. The colored arrows and numbers highlight the ribbons and tubes, which matches the notation in the table. As an example of the analysis of the average ribbon/tube width, the figure presents five different widths measured along the ribbon/tube R1, where we consider the width variation and take measurement points so that these variations are represented in a proportioned manner, *i.e.*, not over- or underrepresenting certain width ranges. This can be seen in R1, where we have one clearly narrower region close to the right end of the tube and we only take one point from there. These five points are then averaged, and we also calculate the standard distribution σ of them to represent the variation of the width, *i.e.*, uniformity of the ribbon/tube: smaller number means more uniform ribbon/tube and higher number more variations on the width along it.

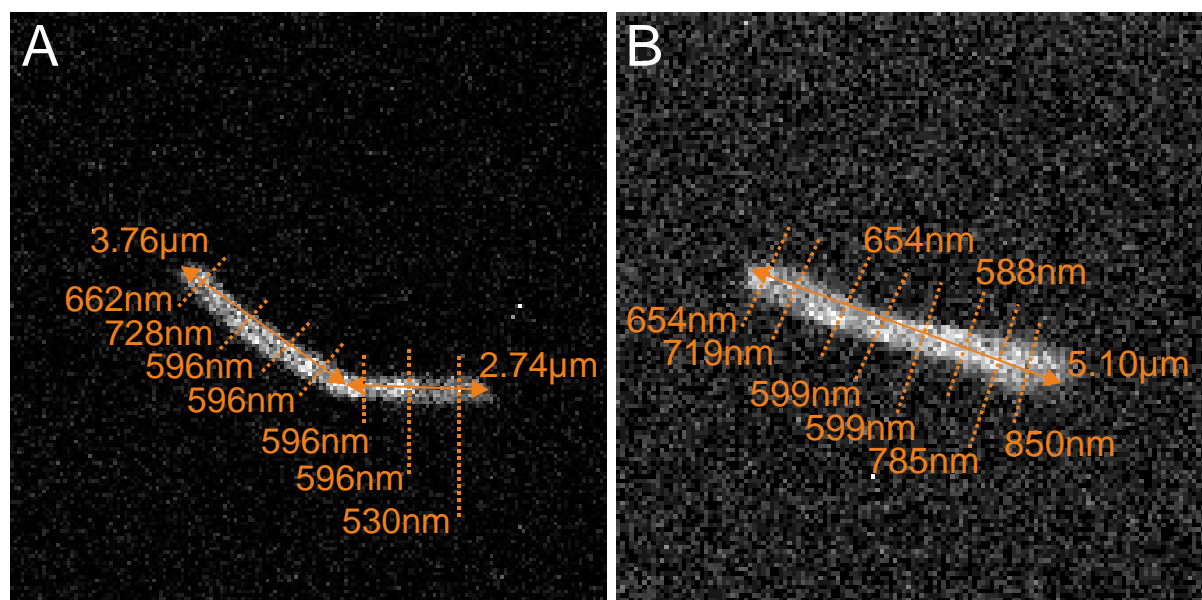


Figure S7. Examples of confocal images for the statistical analysis of the ribbon/tube dimensions. The orange arrows and numbers highlight lengths and widths at various positions along the ribbon/tube. The widths were taken in 0.5 – 1 μm intervals.

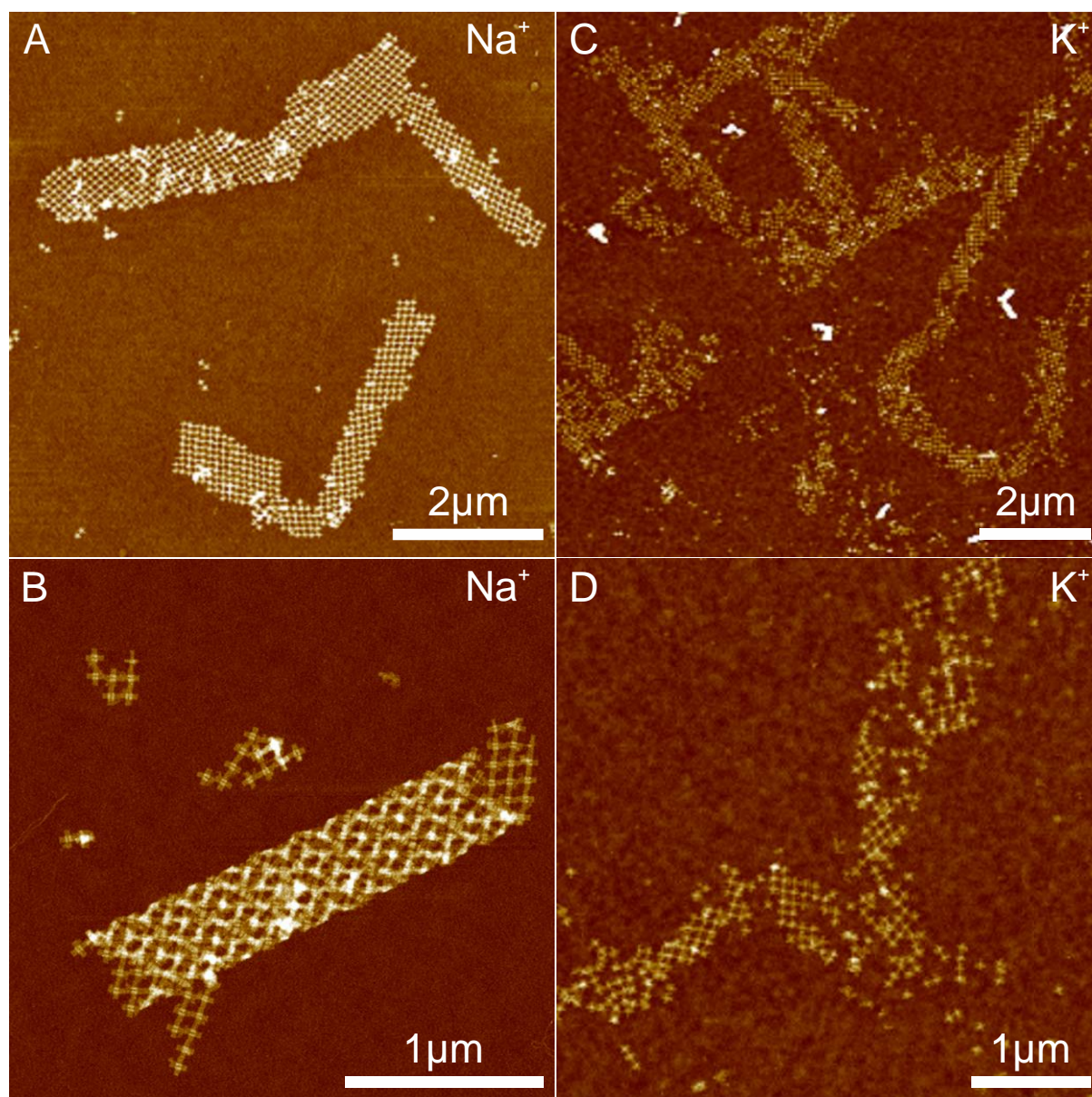


Figure S8. The effect of sodium compared to that of potassium on lattice formation. (A-B) AFM images of ST deposition containing 50 mM Mg²⁺, 5 mM Ni²⁺ and 250 mM Na⁺. (C-D) AFM images of ST deposition containing 50 mM Mg²⁺, 5 mM Ni²⁺ and 250 mM K⁺.

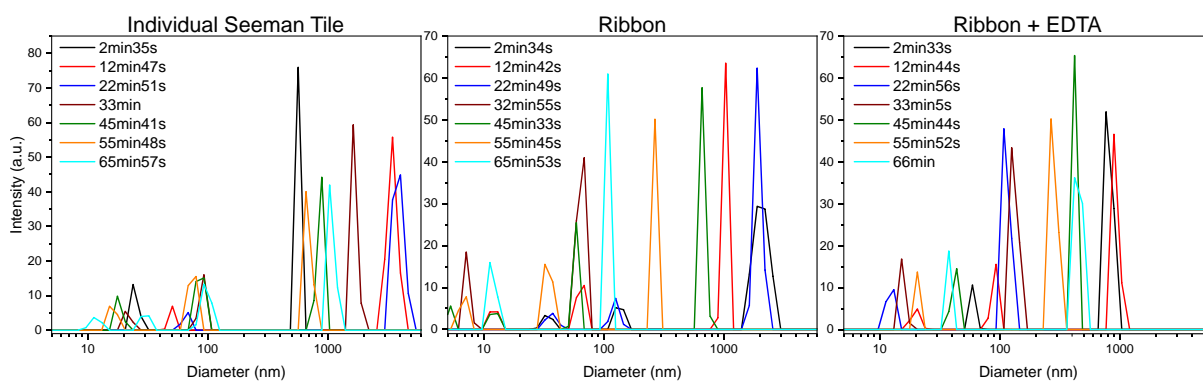


Figure S9. Examples of individual DLS measurements during the ~1 h series of 26 individual measurements. The columns show results for individual Seeman tiles, formation of ribbons, and disassembly of the ribbons by EDTA. The legends show the time of each measurement from the beginning of the series, i.e., beginning of the assembly (ribbon) or disassembly (ribbon + EDTA).

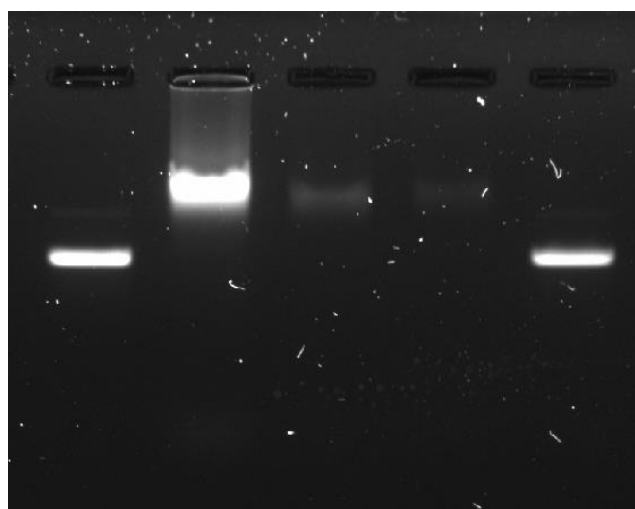


Figure S10. From left to right, gel electrophoresis for scaffold, individual Seeman Tile, ribbon + EDTA, ribbon and other scaffold. Concentration of scaffolds were 15 nM and for origami in others 10 nM. STs were dispersed in the annealing buffer. For ribbons the STs were incubated for 1 h within a cation buffer with 5 mM Ni^{2+} , 50 mM Mg^{2+} and 250 mM Na^+ to allow the formation of ribbons before the gel run. For ribbon + EDTA, 40 mM of EDTA was added to a ready 1 h incubated ribbon solution and let to affect for another 1 h before the gel run. 1 % gel was run with Mupid One Electrophoresis System using 70 V for 1 h. Gel was prestained using SYBR Safe. 1xTAE/12.5 mM MgCl_2 was used as running buffer. 10 μL sample solution with 2 μL of 6x TriTrack as loading buffer was pipetted on the wells. UV image was taken with Biorad Chemidoc MP Imaging system with 10 s exposure.